Polymer 50 (2009) 3145–3152

Contents lists available at ScienceDirect

Polymer

journal homepage: www.elsevier.com/locate/polymer

A visible light photoinitiator system to produce acrylamide based smart hydrogels: $Ru(bpy)_3^{+2}$ as photopolymerization initiator and molecular probe of hydrogel microenvironments

Claudia R. Rivarola, Maria A. Biasutti, Cesar A. Barbero*

Departamento de Química, Universidad Nacional de Río Cuarto, Agencia Postal No 3, 5800 Río Cuarto, Argentina

ARTICLE INFO

Article history:
Received 20 February 2009
Received in revised form
21 April 2009
Accepted 30 April 2009
Available online 12 May 2009

Keywords:
Hydrogel
Photopolymerization
Sensitization

ABSTRACT

A novel visible light bimolecular photoinitiator system (tris(2,2′-bipyridine)ruthenium(II)/*N*,*N*-dimethylaniline) is shown to be able to polymerize *N*-isopropylacrylamide (NIPAM) and 2-Acrylamido-2-Methylpropanesulfonic Acid (AMPS), in aqueous solution, to render high molecular weight polymers and crosslinked gels. The photoinitiator is especially useful to synthesize thermosensitive polymers and gels, because it could be used at temperatures below the phase transition, allowing the polymer chain to grow in its uncoiled state. The polymerization and conversion rates are affected by the structure of the monomer, decreasing in the order NIPAM > AAm > AMPS. The properties of the gels agree with literature data, suggesting that the method is able to produce conventional and smart hydrogels. The microenvironments present near linear polymers and inside crosslinked gels were investigated by measuring fluorescence lifetimes and steady state anisotropy of the metallic complex $(Ru(bpy)_3^{+2}$, present in the solution. Clear effects of the polymer presence on the photophysical properties of the complex are observed. Therefore, the same metallic complex could be used as photoinitiator of vinyl polymerization and as molecular probe to sense the hydrogel microenvironments.

1. Introduction

Synthetic hydrogels have many applications in pharmaceutics, food chemistry, medicine, agriculture and biotechnology [1]. Many hydrogels obtained from synthetic polymers display good biocompatibility and can be used for drug delivery systems [2]. Therefore, the development of new synthetic methods as well of a better understanding of hydrogel properties is of great significance not only in polymer science but also in other fields of materials science.

The synthesis of acrylamide hydrogels is commonly achieved by vinyl polymerization, initiated by redox or thermal initiators. The most common redox initiator pair is persulfate ion ($K_2S_2O_8$)/*N*,*N*,*N*′,*N*′-tetramethylethylenediamine (TEMED) [3]. While the system is reliable and acts at relatively low temperature (20 °C), it has been shown that persulfate anion tends to crosslinking and/or produce chain scission of the hydrogels, as it has been shown for poly(*N*-vinyl-2-pyrrolidone) (PVP) [4,5]. On the other hand, while thermal initiators (e.g. azoisobutyronitrile (AIBN)) do not have aggressive redox components, a certain threshold temperature has to be reached to achieve a reasonable polymerization rate. If that temperature is above the phase transition temperature of the thermosensitive hydrogel, the polymer chains will be growing in its coiled state making the polymerization difficult or impossible. An even worse scenario is present in the case of hydrogels where the gel will be produced in its dehydrated state.

To avoid that, some hydrogels have been prepared by photopolymerization using radiation. A radiation based polymerization allows to control the polymerization duration and to lithographically create patterns on the gels. Using gamma rays has special safety requirements and it was demonstrated that the irradiation dose affects the swelling percent of hydrogel because of the crosslinking density [6]. Ultraviolet radiation has also been used to produce smart hydrogels by photopolymerization [7], but the process is not compatible with biological systems. An initiator system using visible light should be useful. Therefore, water soluble photoinitiator systems for vinyl polymerization, constituted by dyes which absorb visible light, have attracted increasing interest [8–10]. In particular, those based on transition-metal complex have been the subject of several studies [11–14]. One of these systems is composed of tris(2,2′-bipyridine)ruthenium (II) ($Ru(bpy)_3^{+2}$) and co-initiators such as aromatic or aliphatic amines. The system $Ru(bpy)_3^{+2}$–*N*,*N*-dimethylaniline (DMA) was found to be highly efficient to initiate acrylamide polymerization [14].

On the other hand, $Ru(bpy)_3^{+2}$ has been studied because of its good photophysical properties such as strong luminescence,

* Corresponding author. Tel./fax: +54 358 4676 233.
E-mail address: cbarbero@exa.unrc.edu.ar (C.A. Barbero).

0032-3861/$ – see front matter © 2009 Elsevier Ltd. All rights reserved.
doi:10.1016/j.polymer.2009.04.074

moderate excited state lifetime, energy and electron transfer reactions, etc. [15,16]. Luminescence of $Ru(bpy)_3^{+2}$ is assigned to metal-to-ligand charge transfer (MLCT). When the complex is excited, solvent reorganization occurs to stabilize the excited state. Therefore, the fluorescence lifetime is very sensitive to solvent polarity and viscosity [17]. Using those properties, the effect of gel properties (e.g. viscosity) on luminescence, lifetime and polarization properties had been studied in sol–gel [18] and porous vycor glass [19].

The present communication reports that a system based on $Ru(bpy)_3^{+2}$ is able to photoinitiate the chain polymerization of different acrylamides, used in the production of smart hydrogels, like *N*-isopropylacrylamide (NIPAM) and 2-Acrylamido-2-methylpropanesulfonic Acid (AMPS). The polymerization rates (Rp) were measured and found to depend on monomer structure. The polymers are characterized and physicochemical properties of the hydrogels (swelling, phase transition temperature) are measured.

Additionally, the complex is used to probe the hydrogel microenvironments by measuring the influence of the polymers on the fluorescence lifetime and steady state fluorescence anisotropy of the complex. This information allows the understanding of the structural order of linear and crosslinked polymeric systems.

2. Experimental

2.1. Materials

$Ru(bpy)_3Cl_3 \cdot 6H_2O$ (Aldrich) was used as received. *N*,*N*-dimethylaniline (DMA) (Fluka) was vacuum-distilled. Water was triply distilled. Glycerol (Sigma-99%) was used as received. The solutions were deoxygenated by bubbling of pure nitrogen. Monomers: acrylamide (AAm) (Fluka), *N*-isopropylacrylamide (NIPAM) (SP^2) and 2-acrylamido-2-methyl propane sulfonic acid (AMPS) (SP^2) (Scheme 1) were used as received. The crosslinking agent used was *N*,*N*-methylenebisacrylamide (MBAAm) (Aldrich-99%) (Scheme 1).

2.2. Photoinitiator system

The photoinitiator system is bimolecular, composed of an initiator ($Ru(bpy)_3^{+2}$), which absorbs visible light ($\lambda_{max} = 452$ nm), and a co-initiator (DMA) which acts as electron donor. This system was studied in detail previously, using aliphatic and aromatics amines as electron donors, in aqueous solution [14]. By electron transfer reaction between the metal-to-ligand-charge-transfer (MLCT) excited state of the metal complex and the aromatic amine, a radical initiator ($DMA^{\bullet}$) is generated. This radical adds to the vinyl monomer to start chain polymerization (Scheme 2).

2.3. Polymerizations rates

Polymerizations rates were determined by dilatometry, [20] at 25 °C and pH = 3. The conditions of samples solutions were: $[Ru(bpy)_3^{+2}] = 1 \times 10^{-4}$ M, [DMA] = 0.015 M and [monomer] = 0.5 M. Deoxygenated solutions were continuously irradiated with an illumination system based on a Xe-lamp and a high throughput monochromator, set at 450 nm. The internal diameter of the capillary is 0.4 mm and the cell volume is 25 ml. The technique of dilatometry [21] consists of measuring the volume contraction of the solution, due to the lower density of the polymer compared to the monomer, when the monomer is converted into polymer. The volume contraction is determinated through the change in height of dilatometer's capillary. Polymerization rates (Rp) can be determined from the initial slope of volume change versus time of irradiation. The reaction cell is thermostatized at 25 °C by water circulation.

2.4. Conversion of monomers into polymers

To measure conversion rates, solutions of monomers were prepared inside glass tubes and irradiated with visible light during defined time periods. Each solution contains: $[Ru(bpy)_3^{+2}] = 1 \times 10^{-4}$ M, [DMA] = 0.015 M and [monomer] = 0.5 M. The pH was adjusted to 3 by addition of NaOH solution, when needed. Polymerizations were carried out in a merry-go-round Rayonet photochemistry reactor, with the sample in a cylindrical cell with two 4190-Å lamps. The experiments were run by duplicates. Each polymer synthesized at different times was precipitated to determine the percentage of conversion of monomers to polymer. PAAm was precipitated and washed with methanol, while PNIPAM was precipitated by heating the samples above the transition temperature (>35 °C), where the solubility decreases. PAMPS was precipitated in water–acetone (20:80). All precipitates were then filtered and dried in a vacuum oven at 50 °C. The percentage of conversion of monomers agrees (within 2% error) with those obtained by a more cumbersome procedure of ultrafiltration, indicating that polymer loss during precipitation is negligible. The percentage of conversion of monomers (%Conv.) is defined as:

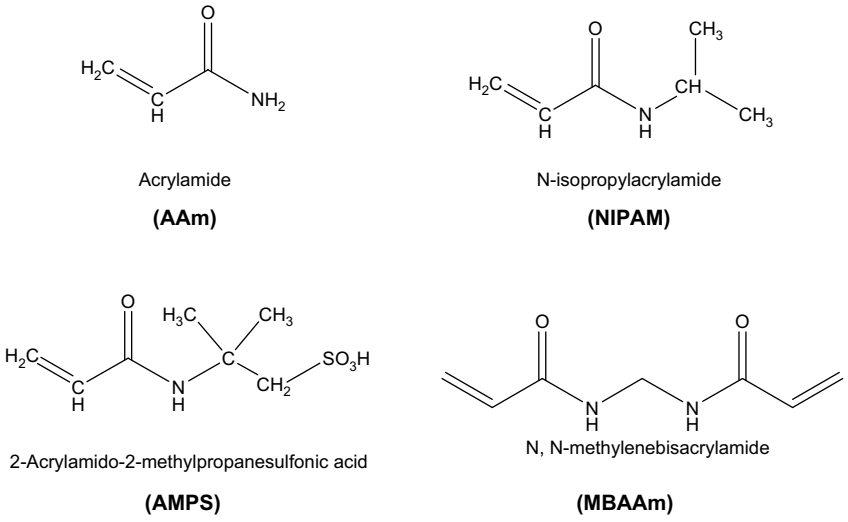

Scheme 1. Structural formulas of monomers used in the present work.

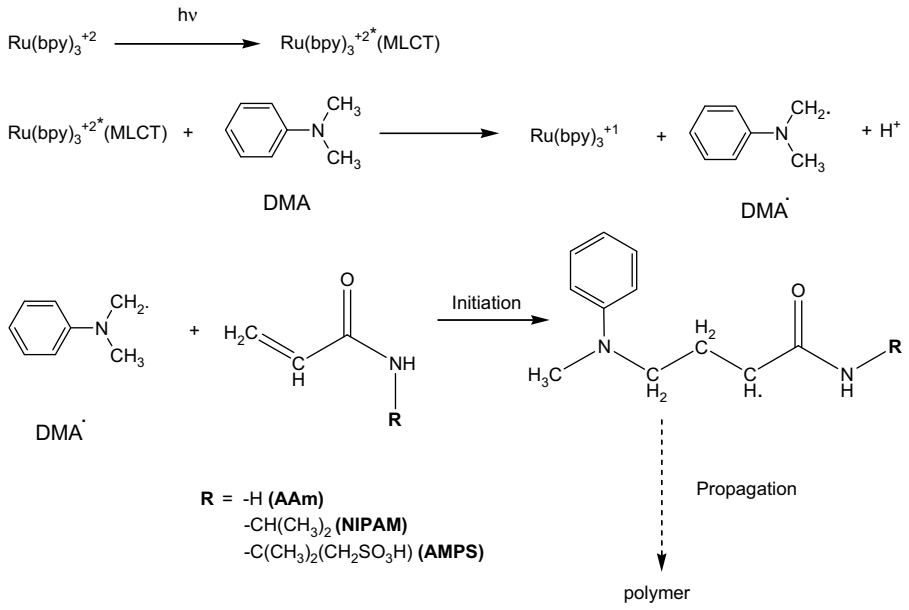

Scheme 2. Mechanism of photopolymerization initiated by radical formation trough a photoinduced electron transfer reaction.

$$\%Conv(t) : \frac{Wo - Wt}{Wo} \times 100$$

Where *Wt* is the weight of polymer obtained at each time *t* of irradiation, and *Wo* is the initial weight of monomer.

2.5. Photochemical synthesis of linear polymers

A set of solutions, with the same concentrations of reagents than in the case of kinetic studies, were prepared. The solutions were then irradiated 5 and 10 min, for NIPAM and AMPS solutions, respectively, so all polymers had approximately 5% conversion. The conversions were restricted to 5% to avoid large changes in viscosity which could produce variations in the molecular weight of the polymers.

2.6. Photochemical synthesis of gels

To produce gels, a 2% (mol/mol of monomer) concentration of a crosslinker (MBAAm), was added to the polymerization solution. The concentration of the other reagents was the same than in the case of linear polymers. The gels were immersed in flowing distilled water to remove unreacted reagents. Complete removal of metallic complex was verified by UV–vis spectroscopy of the washing solution.

2.7. Molecular weight determination

The molecular weights of linear polymers synthesized to 5% of conversion were determined by static light scattering (SLS) in a Malvern 4700 device with an argon-ion laser operating at 488 nm. The SLS data were treated using Zimm's double extrapolation method. Molecular weight determinations were conducted at 20 °C in THF. A high-precision refractometer (Abbe 60) was used to measure the *dn/dC* values at 488 nm.

2.8. FTIR spectroscopy

FTIR spectra were measured in a Impact 400 spectrometer (Nicolet) by transmission in KBr. The polymers were dried under vacuum before measurement.

3. Measurement of swelling

The swelling percentage was determined gravimetrically. Gels prepared with cylindrical shapes, were immersed in distilled water to remove low molecular weight substances and then dried to constant weight. Dried hydrogels were left in aqueous solution at room temperature (20 °C). After a certain time *t*, the gels are taken out of water, the excess water is wiped and the gels are weighed. The swelling percentage is calculated as:

$$\%Swelling = \left[\frac{(Wt - Wo)}{Wo}\right] \times 100$$

where *Wo* is the dried initial weight of gel at time $t = 0$, and *Wt* is the weight of swollen gel at time *t*.

3.1. Phase transition temperature

The phase transition temperature of PNIPAM was determined by visual observation of gel volume and transparency while heating, [22] or by finding the maxima in the heating curve measured by differential scanning calorimetry (TA Instruments 2090).

3.2. Fluorescence lifetimes and anisotropy experiments

Fluorescence lifetimes (τ) were determined by the time-correlated single-photon-counting technique using an OB-900 Edinburgh Instruments instrument. The cell holder was thermostatized by water circulation. The sample was irradiated at 370 nm and the peak emission wavelength was observed at 610 nm. Steady state fluorescence anisotropy measurements $<r>$ were determined by Hitachi 2500 spectrofluorometer, with Glan-Thomson polarizers. These experiences were carried out only at room temperature, with the purpose of comparing with the results of lifetimes experiences. Fluorescence anisotropy value was obtained using the expression $<r> = I_{VV} - G \cdot I_{VH}/(I_{VV} + 2\,G \cdot I_{VH})$, where I_{VV} and I_{VH} are the vertically and horizontally polarized emission components (spectrum) after excitation by vertically polarized light and *G* is the sensitivity factor of the detection system.

3.3. Molecular calculations

The structure of the polymers, in contact with the $Ru(bpy)_3^{+2}$ probe, was calculated using the Merck Molecular Field 94 (MMF94) method built in ChemDraw 11 (CambridgeSoft). A small portion (five monomer units) of the polymer chain was drawn and its energy minimized along with that of the complex.

4. Results and discussion

4.1. Kinetic of vinylic polymerization

The polymerization rates (Rp) of the monomers, were determined by dilatometry. The change in height of the liquid column inside the dilatometer's capillary is related with the solution volume change. In Fig. 1, it can be seen the height contraction in the capillary as a function of irradiation time during the polymerization. Typically, a period of induction (between 5 and 10 min) is observed due to the presence of oxygen in the solution. The maximum linear contraction of the fluid in the capillary (ca. 16%) corresponds to ca. 0.08% contraction of the polymerization solution. The initial slope of the graph represents Rp, which is determined for NIPAM, AMPS and acrylamide (AAm).

Comparing the Rp values measured for NIPAM and AMPS with that measured for AAm (Table 1), it can be seen that the photoinitiator system is able to polymerize NIPAM and AMPS. However, the polymerization rate depends on the functional group substitution on the nitrogen of the amide group.

It seems that the isopropyl group in NIPAM stabilizes the radical by hyperconjugation effect, thereby increasing the rate. In the case of AMPS two effects could be operative to reduce Rp: i) the inductive (electron withdrawing) effect of the sulfonate group; ii) coulombic repulsion effects between the sulfonate groups present in the growing chain and the monomer. It is likely that the later effect is more important.

4.2. Conversion rates

The same trend of reactivity is observed when the degree of conversion of monomer into polymer is measured as a function of time (Fig. 2). As it can be seen, the conversion rates, follows the order NIPAM > AAm > AMPS.

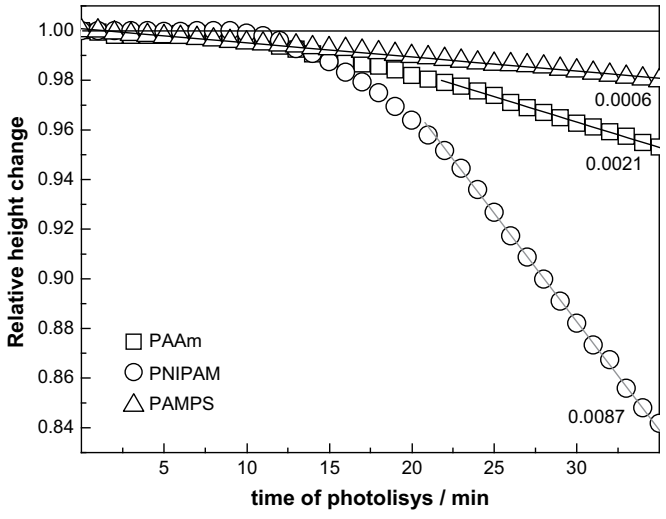

Fig. 1. Dilatometric measurements of polymerization rates at 25 °C and pH = 3. Photoinitiator system: $Ru(bpy)_3^{+2}$ (10^{-4} M) – DMA (0.015 M). Monomer concentration: 0.5 M (AAm, NIPAM or AMPS).

Table 1
Relatives polymerization rates determined by dilatometry, at 25 °C and pH = 3.

Systems	Rp (relative)
AAm	1
AMPS	0.3
NIPAM	4.1

4.3. Polymer characterization and hydrogel behavior

While the photoinitiator system seems able to polymerize AMPS and NIPAM, to produce both linear polymers and hydrogels, it is important to know if the materials produced are equivalent to those produced by more common methods, like thermal initiation. It is possible that secondary reactions alter the primary structure or secondary structure of the polymers. Therefore, the polymers were characterized and the behavior of the hydrogels studied.

4.4. FTIR spectroscopy

FTIR spectra of the polymers reveal characteristics absorption bands of acrylamides (Fig. 3). Both in PNIPAM and PAMPS show bands at 2974 and 2881 cm^{-1} (–CH_3 symmetric and asymmetric stretching), 1660 and 1538 cm^{-1} (N–H stretching amide I and II) and the isopropyl methyl deformation bands at 1386 and 1367 cm^{-1} [23,24]. Additionally, in PAMPS several characteristics bands of the sulfonic group are present: 1192–1040 cm^{-1} (asymmetric and symmetric O═S═O stretching) and 630 cm^{-1} (st. C–S) [24,25]

Therefore, the structure of the polymer monomer units seems not to be altered by the polymerization procedure.

4.5. Molecular weight

The molecular weight of linear PNIPAM was determined to be of 1.12×10^6 g/mol. The value is in order of those reported for acrylamide polymerization with radiation [26], suggesting that the termination reactions with DMA• are inhibited. Alternatively, it could be envisaged that carrying out the polymerization in uncoiled state produces higher molecular weights due to the free access to the extreme of the growing chain [27]. Obviously, most thermally initiated polymerizations are carried out above the phase transition temperature, where the chains are produced in a coiled state with lower extreme mobility. In the case of PAMPS, the molecular weight

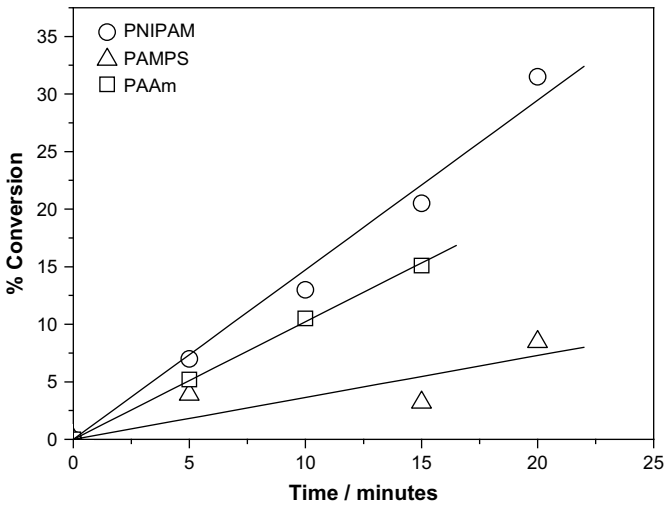

Fig. 2. Conversion of monomer into polymer as a function of irradiation time.

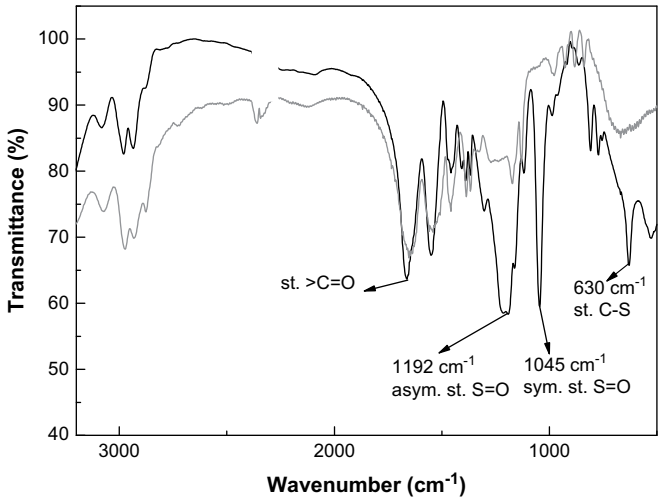

Fig. 3. FTIR spectra of PNIPAM (grey line) and PAMPS (black line). Both polymers were produced by photopolymerization.

values could be affected by interactions between charged chains. However, a value of 5.6×10^5 g/mol was measured. The value is in agreement with published data on PAMPS, [28] but it is lower than in the case of PNIPAM, probably due to interactions of the growing chains [29]. In any case, it seems evident that the photopolymerization method proposed here is able to produce high molecular weight polyacrylamides.

4.6. Swelling of PNIPAM and PAMPS gels

Both PNIPAM and PAMPS hydrogels swell when immersed in water (Fig. 4), in agreement with previous reports.

The swelling was measured below the phase transition temperature of PNIPAM (see below) where the polymer is in its uncoiled state. PNIPAM swells slowly to a constant value of ca. 120% due to the hydrogen bonding interaction of water with the amide group. On the other hand, PAMPS swells very rapidly to ca. 4000% before hydrogel disintegration. Such high swelling level is due to the hydrogen bonding of water with the sulfonate groups and to the entropic effect of mobile counterions. In the collapsed state, counterions have lower mobility because they reside close to the

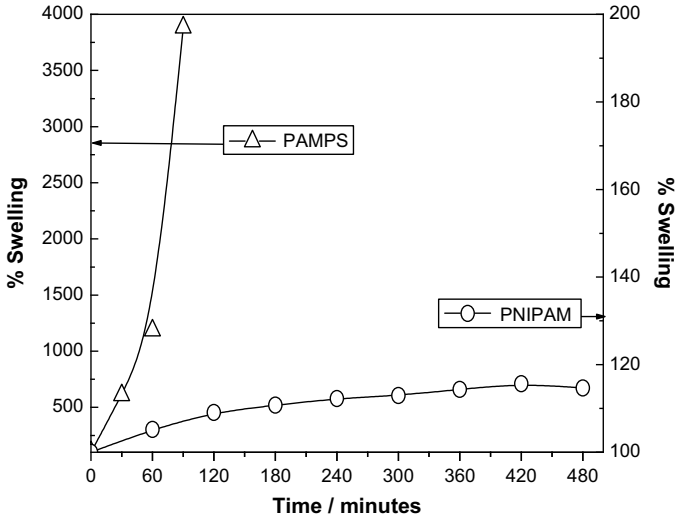

Fig. 4. Swelling of PAMPS and PNIPAM crosslinked gels in water at 20 °C.

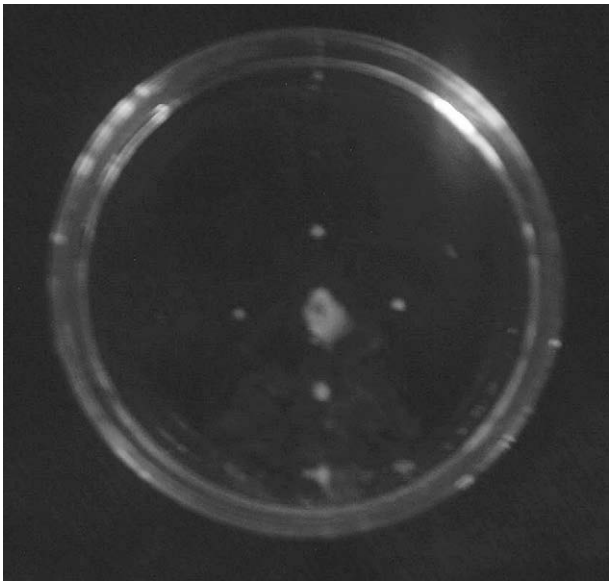

Fig. 5. Photograph of PNIPAM gel dots on the lower surface of a glass Petri dish, produced by photopolymerization. The photograph was taken with the dish heated at 40 °C.

sulphonate groups. By incorporation of water, aqueous domains are built inside the hydrogel where mobile cations could increase its entropy by translation in the aqueous solution. Such entropy increase is the main driving force of the swelling in PAMPS.

4.7. Phase transition temperature of photochemically produced PNIPAM hydrogel

The volume changes of a PNIPAM hydrogel upon changing the temperature can be seen to occur at 32–33 °C. The value agrees with those reported in the literature for PNIPAM hydrogels produced using a thermal initiator [30].

4.8. Image formation by photopolymerization

The formation of hydrogel patterns on surfaces is of great interest towards biomedical applications of the materials [31,32]. Indeed, the photopolymerization procedure described above can be used to produce pattern of the smart hydrogels (Fig. 5). Using a sealed set-up where a dotted pattern (a central spot and four diffraction spots) of blue (472 nm) light (*see supl. inf.*) which is shine onto a photopolymerization solution, a clear pattern of gel dots is produced which corresponds to the regions of highest illumination.

The dots remain attached to the bottom glass surface of a Petri dish. They are not visible at 25 °C but become visible when the dish is heated above the transition temperature of PNIPAM (ca. 32 °C). Above that temperature the smart hydrogel structure collapses and its refractive index becomes higher than that of the surrounding solution, making the dots visible. This result suggests that images made of smart hydrogels which are sensitive to environmental

Table 2
Lifetime of $Ru(bpy)_3^{+2}$ in aqueous solution, NIPAM-monomer (0.5 M) and PNIPAM solution (5% w/v), at different temperatures.

Temperature	Aqueous solution (τ/ns)	NIPAM (τ/ns)	PNIPAM (τ/ns)
25 °C	418	460	435
30 °C	384	413	387
37 °C	352	364	–

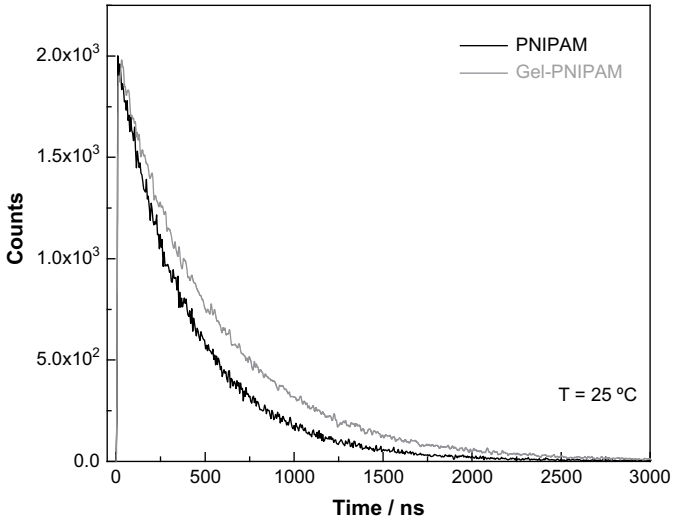

Fig. 6. Fluorescence decay curves of $Ru(bpy)_3^{+2}$ in PNIPAM and Gel-PNIPAM, extracted at 5% conversion, at 25 °C. The excitation wavelength was 370 nm and the emission was observed at 610 nm.

parameters (e.g. temperature for PNIPAM hydrogels), can be produced using the photopolymerization method.

The initiator system remains inside the system but can be completely removed ($<10^{-6}$ M as determined by UV–vis spectroscopy) from the hydrogels by washing with water. This fact suggests that sequential formation of interpenetrated hydrogels could be made by addition of another monomer and subsequent photopolymerization [33].

Moreover, the well known photophysics of $Ru(bpy)_3^{+2}$ allows to use it as probe to monitor the polymer microenvironments [8–10]. Besides the fundamental interest to understand better the interactions of polymer chains with molecules, this complex has been used as a stable fluorescence tracer in biological systems [34,35]. Additionally, the complex could be used as molecular analogue of organometallic anticancer drugs [36]. Therefore, the understanding of its interactions with acrylamide polymers is important when smart hydrogels are used in drug release devices or biomaterials.

4.9. Study of polymer microenvironments using $Ru(bpy)_3^{+2}$ as probe

4.9.1. Fluorescence lifetime of $Ru(bpy)_3^{+2}$ in different polymeric systems

In all cases, the lifetimes measured show a first-order decay. Therefore, the τ of complex is dependent on temperature of system [15,16]. In Table 2 are shown the lifetimes (τ) of $Ru(bpy)_3^{+2}$ determined in the following media: aqueous solution, solution of the monomer and in a solution of linear PNIPAM.

It could be observed that τ increases from aqueous to monomer solution, but in the polymer solution, τ has similar values than in pure water. At each temperature, the same tendency was observed.[1] It is likely that the τ of $Ru(bpy)_3^{+2}$ is larger in NIPAM solution than in water due to the higher microviscosity of the 0.5 M solution. But in a solution of linear PNIPAM, lifetimes (τ) show values similar to those in pure water. One explanation is that while the macroscopic viscosity of the solution is higher in a PNIPAM than in a NIPAM solution, $Ru(bpy)_3^{+2}$ seems to be located in aqueous domains of free water away from the polymer chains. Alternatively, the vinylic part of the monomer, absent in the polymer, could have a π–π interaction with the aromatic ring in the bipyridil groups.

In Fig. 6, it can be seen the decay curve observed in linear and crosslinked PNIPAM polymers. The lifetime (τ) of $Ru(bpy)_3^{+2}$ in the presence of linear (not crosslinked) PNIPAM solution, is smaller than the one measured in PNIPAM gel, at all temperatures.

In Table 3, the τ of $Ru(bpy)_3^{+2}$ inside the crosslinked and uncrosslinked polymers of NIPAM is presented.

It seems that the crosslinked structure of the gel immobilizes the complex, restraining its movements. Therefore, a more rigid environment is detected through an increment of the complex excited state lifetime.

In Table 4, the τ of $Ru(bpy)_3^{+2}$ in the presence of crosslinked or uncrosslinked polymers of AMPS is shown. Surprisingly, the lifetime (τ) decreases when the complex is inside the crosslinked gel, compared with linear PAMPS, to values close to those measured in water (see Table 2). It seems that neighboring sulphonate groups in linear PAMPS repel electrostatically, forcing the flexible chain to assume a rod like shape, where the cationic probe could interact with the sulfonate groups. Therefore, the probe sees a more rigid environment. On the contrary, the crosslinked structure of the PAMPS gel precludes an extended conformation of the chains and segregates the complex to the water pools where it sees a less rigid microenvironment. Accordingly, the τ values show values similar to those measured in pure water.

A comparison of the data shown in Tables 3 and 4 suggests that the lifetime (τ) of $Ru(bpy)_3^{+2}$ in a solution of linear PAMPS is higher than in a solution of linear PNIPAM, probably because electrostatic interactions exist between the complex and the anionic (sulphonate) groups, thereby decreasing the mobility of the probe. On the other hand, the τ values observed in PAMPS gel are lower than those measured in the PNIPAM gel, indicating that the probe is freer to move in the water domains inside the gel. This is reasonable because PAMPS gel shows a higher degree of swelling than PNIPAM gel, therefore contains larger water pools. Alternatively, the complex could interact strongly to the uncharged PNIPAM matrix by hydrophobic forces between the large complex and the alkyl groups in the polymer chain.

To understand better the effect of microenvironment on the luminescence behavior, we perform fluorescence anisotropy measurements.

4.9.2. Fluorescence anisotropy of $Ru(bpy)_3^{+2}$ in different systems

Anisotropy measurements are based on the principle of photoselective excitation of fluorophores by polarized light. Fluorophores preferentially absorb photons whose electric vectors are aligned parallel to the transition moment of the fluorophore, which has a defined orientation with respect to the molecular axis. In an isotropic solution, the fluorophores are oriented randomly. Upon

Table 3
Lifetime of $Ru(bpy)_3^{+2}$ in presence of linear or crosslinked PNIPAM.

Temperature	PNIPAM (τ/ns)	Gel-PNIPAM (τ/ns)
25 °C	403	542
30 °C	347	453
37 °C	#	#

Above phase transition.

Table 4
Lifetime of $Ru(bpy)_{23}^{+2}$ in linear and crosslinked PAMPS.

Temperature	PAMPS (τ/ns)	Gel-PAMPS (τ/ns)
25 °C	506	441
30 °C	435	389
37 °C	374	337

[1] Since PNIPAM has a phase transition temperature at ca. 32 °C, τ could not be measured above this temperature, because the light is scattered by the coiled polymer.

Table 5
Steady state anisotropy $<r>$ values of $Ru(bpy)_3^{+2}$ in glycerol, by excitation at different wavelengths, at 25 °C.

λ_{exc} (nm)	$<r>$
400	0.014 ± 0.005
450	0.009 ± 0.001
465	0.044 ± 0.001
475	0.015 ± 0.002
490	0.017 ± 0.001
510	0.021 ± 0.002

excitation with polarized light, one selectively excites those fluorophore molecules whose absorption transition dipole is parallel to the electric vector of the excitation. Emission also occurs with the light polarized along a fixed axis in the fluorophore. The relative angle between these moments determines the maximum measured anisotropy $<r>$. Rotational diffusion decreases the measured anisotropy to values lower than the maximum theoretical values. Such diffusion occurs during the lifetime of the excited state and displaces the emission dipole of the fluorophore. Since fluorophores in non-viscous solution typically display anisotropies near zero, measurement of anisotropy provides information on probe environment viscosity [37].

First, a solution of $Ru(bpy)_3^{+2}$ in glycerol, was excited at different wavelengths to determine the excitation wavelength where the probe presents the maximum anisotropy value. In Table 5, the excitation wavelength and the $<r>$ calculated by $Ru(bpy)_3^{+2}$ in glycerol, are listed. The maximum anisotropy occurs by excitation at 465 nm, which is similar to that observed for the complex in porous vycor glass (PVG) [19] and in ethanol glass (77 K), where the fundamental anisotropy (r_0) value was 0.2 [38]. The peak emission wavelength was observed at 610 nm.

Then, the fluorescence anisotropy was also measured in different polymer environments exciting at 465 nm. In Table 6, the results of $<r>$ and τ of $Ru(bpy)_3^{+2}$ in different media are presented. It can be seen that the fluorescence anisotropy of the complex is sensitive to the changes in the probe microenvironment.

The $<r>$ value in water (least viscous) and glycerol (most viscous), is shown in order to present extreme values of anisotropy. The polymer systems show intermediate values of $<r>$, being the ones obtained for gel-PNIPAM and linear PAMPS the largest ones. The tendency is similar to those presented in the fluorescence decay lifetime. The anisotropy values are higher in crosslinked NIPAM than in linear NIPAM because the probe movements are more restricted. It should be remembered that, below the phase transition temperature, the PNIPAM hydrogel contains a significant amount of water which interacts by hydrogen bonding with the amide groups. For this reason, inside the gel, the probe molecules are now located inside the gel seeing a constrained environment.

Another type of constraint of the probe movements occurs by electrostatic interaction between anionic (sulfonate) groups in linear PAMPS and the cationic probe. This is evident in a larger anisotropy. On the other hand, the crosslinking of PAMPS produces a decrease of both the decay time and anisotropy, suggesting that

Table 6
Anisotropy $<r>$ values and lifetimes (τ) of $Ru(bpy)_3^{+2}$ in different media. $\lambda_{exc} = 465$ nm.

System	$<r>$	τ (ns)
Water	0.004	351
Gel-PAMPS	0.006	441
PNIPAM	0.007	403
Gel-PNIPAM	0.012	542
PAMPS	0.012	506
Glycerol	0.044	956

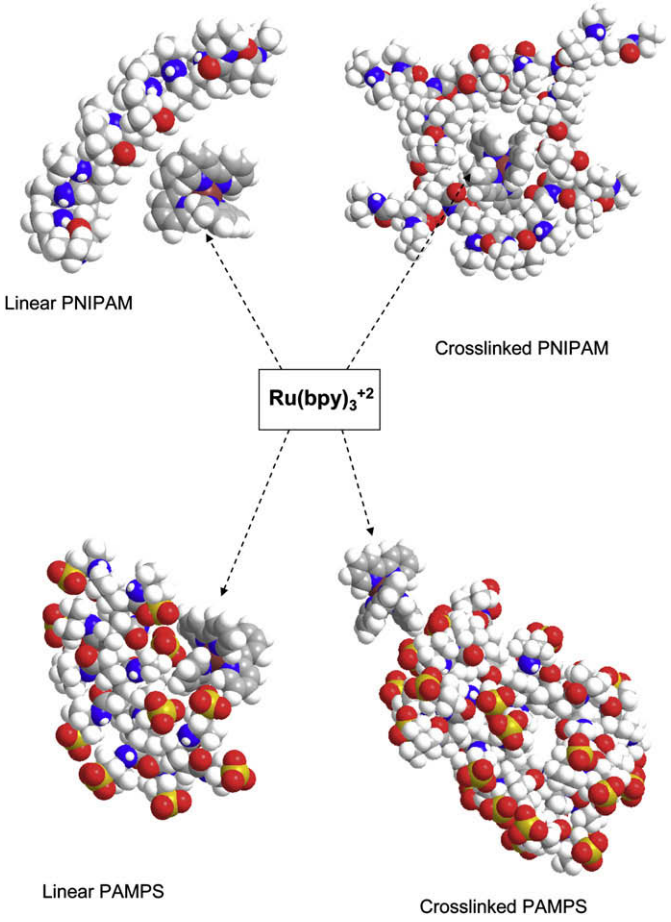

Scheme 3. Energy minimized polymer conformations and its interactions with the fluorescent probe. The Ru atoms are shown in dark red, oxygen in red, sulfur in yellow, nitrogen in blue and carbon in grey. For sake of clarity, the hydrogen atoms are not drawn.

the probe is freer to move, being located in aqueous domains, outside the crosslinked regions. In the gel, the repulsive interactions between sulphonate groups are opposed by the covalent crosslinks, producing less extended structure. It is likely that the close packing of the negative charges allows only a few cationic probes molecules (much larger) to interact with the negative charges, being the rest compensated by small mobile ions. Most of the probe molecules are then situated in the aqueous domains of the gel, freer to move.

Taking these results into account, it is possible to draw a structure of the polymers in solution and propose the structures that are adopted by these polymer systems (Scheme 3). As it can be seen, only in crosslinked PNIPAM gels the $Ru(bpy)_3^{+2}$ probe is close to the polymer matrix, while in all other cases is present in aqueous environments far from the polymer chains.

5. Conclusions

A new photoinitiator system consisting of $Ru(bpy)_3^{+2}$ and DMA, is shown to be able to polymerize substituted acrylamides (NIPAM and AMPS), commonly used to produce smart hydrogels. The method could be used at temperatures below the phase transition temperature, (ca. 32 °C for PNIPAM) allowing the polymer to grow in its uncoiled state. Accordingly, high molecular weight polymers can be obtained. Using the photopolymerization method described above, images made of thermoresponsive PNIPAM hydrogels were easily produced.

The photophysics of the metallic complex $Ru(bpy)_3^{+2}$ is used to monitor the microenvironments near polymer chains or inside polymer gels. Linear PAMPS interacts more strongly with the complex than linear PNIPAM, as shown in decreasing lifetimes and higher anisotropy. However, crosslinked PAMPS gel seems to show the reverse effect being the complex freer to move than in PNIPAM gel. This is likely to be related to the higher swelling ratio of PAMPS to PNIPAM which allows larger water pools to be present in gel-PAMPS.

Acknowledgements

The work has been funded by FONCYT, CONICET and SECYT-UNRC. The authors are permanent research fellows of CONICET. Helpful comments by the reviewers are gratefully acknowledged.

Appendix. Supplementary data

Photographs of patterns of thermoresponsive PNIPAM hydrogels produced by the photopolymerization method and of the experimental set-up. Supplementary data associated with this article can be found, in the online version, at doi:10.1016/j.polymer.2009.04.074.

References

[1] Dhal PK, Huval CC, Holmes-Farley CR. Ind Eng Chem Res 2005;44(23):8593–604.
[2] Hoffman A. Adv Drug Delivery Rev 2002;54(1):3–12.
[3] Guilherme M, da Silva R, Rubira A, Geuskens G, Muniz E. Reactive Funct Polym 2004;61(2):233–43.
[4] Anderson C, Rodríguez F, Thurston D. J Appl Polym Sci 1979;23(8):2453–62.
[5] Tenhu H, Sundolm F. Macromol Chem 1984;185(9):2011.
[6] Kaplan Can H, Denizli B, Kavlak S, Guner A. Radiat Phys Chem 2005;72(4):483–8.
[7] Dong L, Agarwal AK, Beebe DJ, Jiang H. Nature 2006;442(3):551–4.
[8] Encinas M, Lissi E, Rufo A, Previtali C. J Polym Sci Part A Polym Chem 1990;32(9):1649–55.
[9] Rodrigues M, Catalina F, Neumann M. J Photochem Photobiol A Chem 1999;124(1–2):29–34.
[10] Costela A, Garcia-Moreno I, Garcia O, Sastre R. J Photochem Photobiol A Chem 2000;131(1–3):133–40.
[11] Iwai K, Uesugi M, Takemura F. Polym J 1985;17(9):1005–11.
[12] Iwai K, Uesugi M, Sakabe T, Hazama C, Takemura F. Polym J 1991;23(6):757–63.
[13] Pizzocaro C, Bolte M. Polyhedron 1993;12(8):855–8.
[14] Rivarola CR, Bertolotti S, Previtali C. J Polym Sci Part A Polym Chem 2001;39(24):4265–73.
[15] Juris A, Balzani V, Barigelleti F, Campagna S, Belser V, Zelewsky A. Coord Chem Rev 1988;84(C):85–277.
[16] Caspar J, Meyer T. J Am Chem Soc 1983;105(17):5583–90.
[17] Sakka S, Kozuka H, editors. Handbook of sol gel science and technology. New York: Kluwer Academic Publishers; 2005. p. 474.
[18] Matsui K, Momose F. Chem Mater 1997;9(11):2588–91.
[19] Shi W, Wolfgang S, Strekas T, Gafney HJ. Phys Chem 1985;89(6):974–8.
[20] Cowie JMG. Polymers: chemistry & physics of modern materials. Chichester: Stanley Thornes; 1998.
[21] Odian G. Principles of Polymerization, 2nd ed. New York: Wiley-Interscience; 1981.
[22] Yildiz B, Isik B, Kis M. React Func Polym 2002;52(1):3–10.
[23] Alarcon C, Farhan T, Osborne V, Huck W, Alexander C. J Mater Chem 2005;15(21):2089–94.
[24] Silverstein RM, Webster FX, Kiemle D. Spectrometric identification of organic compounds, 7th ed. New York: Wiley; 2005.
[25] Durmaz S, Okay O. Polymer 2000;41(10):3693–704.
[26] Wada T, Sekiya H, Machi S. J Appl Polym Sci 2003;20:3233–40.
[27] Flory PJ. Principles of polymer chemistry. Cornell: Cornell University Press; 1953.
[28] Kruczała K, Szczubiałka K, Łancucki L, Zastawny I, Gora-Marek K, Dyrek K, et al. Spectrochim Acta Part A 2008;69:1337–43.
[29] Budanova YE, Shvetsov OK, Maer ZhA. Russ J Appl Chem 2001;74:1215–9.
[30] Chee C, Rimmer S, Soutar I, Swanson L. Polymer 2001;41:5079–87.
[31] Yu T, Ober CK. Biomacromolecules 2003;4(5):1126–31.
[32] Lee W, Choi D, Lee Y, Kim D-N, Park J, Koh W-G. Sens Actuators B 2008;129(2):841–9.
[33] Kızılel S, Sawardecker E, Teymour F, Pérez-Luna VH. Biomaterials 2006;27(8):1209–15.
[34] Marcon G, Carotti S, Coronnello M, Messori L, Mini E, Pierluigi Orioli P, et al. J Med Chem 2002;45(8):1672–7.
[35] Dyson PJ, Sava G. Dalton Trans 2006;(16):1929–33.
[36] Laïb S, Fellah BH, Fatimi A, Quillard S, Vinatier C, Gauthier O, et al. Biomaterials 2009;30(8):1568–77.
[37] Lakowicz JR. Principles of fluorescence spectroscopy, 3rd ed. Singapore: Springer; 2006.
[38] Felix F, Ferguson J, Gudel H, Ludi A. J Am Chem Soc 1980;102(12):4096–102.